Geophysical Prospecting EAGE EUROPEAN ASSOCIATION OF GEOSCIENTISTS & ENGINEERS

Geophysical Prospecting, 2012, **60**, 239–254 doi: 10.1111/j.1365-2478.2011.00979.x

Seismic time-lapse effects of solution salt mining – a feasibility study

Guy Drijkoningen[1]*, Guus van Noort[1], Rob Arts[1], Joren Bullen[2] and Jan Thorbecke[1]

[1]*Department of Geotechnology, Delft University of Technology, Stevinweg 1, 2628 CN Delft, the Netherlands, and* [2]*NedMag Industries Mining & Manufacturing B.V., Billitonweg 1, 9640 AE Veendam, the Netherlands*

Received May 2010, revision accepted March 2011

ABSTRACT

This article addresses the question whether time-lapse seismic reflection techniques can be used to follow and quantify the effects of solution salt mining. Specifically, the production of magnesium salts as mined in the north of the Netherlands is considered. The use of seismic time-lapse techniques to follow such a production has not previously been investigated. For hydrocarbon production and CO_2 storage, time-lapse seismics are used to look at reservoir changes mainly caused by pressure and saturation changes in large reservoirs, while for solution mining salt is produced from caverns with a limited lateral extent, with much smaller production volumes and a fluid (brine) replacing a solid (magnesium salt).

In our approach we start from the present situation of the mine and then study three different production scenarios, representing salt production both in vertical and lateral directions of the mine. The present situation and future scenarios have been transformed into subsurface models that were input to an elastic finite-difference scheme to create synthetic seismic data. These data have been analysed and processed up to migrated seismic images, such that time-lapse analyses of intermediate and final results could be done.

From the analyses, it is found that both vertical and lateral production is visible well above the detection threshold in difference data, both at pre-imaging and post-imaging stages. In quantitative terms, an additional production of the mine of 6 m causes time-shifts in the order of 2 ms (pre-imaging) and 4 ms (post-imaging) and amplitude changes of above 20% in the imaged sections. A laterally oriented production causes even larger amplitude changes at the edge of the cavern due to replacement of solid magnesium salt with brine introducing a large seismic contrast. Overall, our pre-imaging and post-imaging time-lapse analysis indicates that the effects of solution salt mining can be observed and quantified on seismic data. The effects seem large enough to be observable in real seismic data containing noise.

Keywords: Modelling, Monitoring, Numerical study, Seismics, Time-lapse.

1 INTRODUCTION

In the north of the Netherlands the rare magnesium salt minerals carnallite and bischofite are extracted from the subsurface at about 1.6 km depth. The occurrence of bischofite is geographically limited and in the northern part of the Netherlands the bischofite is of a unique purity. The magnesium salts are mined through solution-based methods, initially via conventional solution mining, later via squeeze mining. It is perceived that the salts are produced from caverns around the injection/production wells.

*E-mail: g.g.drijkoningen@tudelft.nl

Effects of salt mining

The salt mining takes place in an urbanized area, with the consequence that precise control of the solution mining is getting more and more desired. One of the undesired effects of the mining is subsidence of the surface. Various models of the mine and overburden have been developed that could explain this subsidence but these ideas are very much driven by conceptual models of the subsurface and not by quantitative subsurface data. Even for the mine itself, only a qualitative notion exists for the geometry of the salt caverns, if caverns at all. In our view, a better understanding of the mine (i.e., the development of the cavity geometry in time) may lead to more controlled and effective salt production, allowing surface subsidence to be kept to a minimum.

The added value of seismic monitoring

During the last decades, seismic monitoring of the subsurface has become more popular in the hydrocarbon industry (see also Calvert 2005) and CO_2-storage projects (see e.g., Arts *et al.* 2004). The technique allows observing changes in the subsurface, which are caused by the production or injection of respectively hydrocarbons and CO_2. The technique has proven adequate in numerous examples to discriminate between producing and non-producing zones in oil and gas production or to track the spreading of injected CO_2 in a reservoir. More sophisticated prestack data analysis can potentially discriminate between pressure and saturation effects (Landrø 2001). Application of the latter technique is not standard and requires proper calibration to rock physics coming from log and core measurements.

In general, seismic monitoring is mostly established in time-lapse mode, i.e., surveys carried out at discrete times (months, years). Via comparison and analysis of differences, conclusions can be drawn on the changes of the reservoir itself. A very striking feature of such analyses is that it may happen that while the image itself does not reveal so much structure or too much structure, the difference may be significant. This has been demonstrated for carbonate reservoirs (see Calvert 2005).

For solution salt mining, a similar approach can be taken to identify produced salt zones in time. For pure imaging purposes, the seismic technique is not used for salt mining, since the presence of magnesium salts cannot clearly be distinguished. Combined with the relatively high cost, the added value for imaging has not been demonstrated so far. However, the impact on the improved understanding of the production process of a salt may make it worthwhile to invest in seismics for monitoring purposes. This study is meant as a feasibility study to assess whether technically the cavern growth in time can be detected in seismic time-lapse mode.

Adopted methodology

In this study the effects of production will be related to the changes in geometry and properties of the brine caverns. The ability of time-lapse seismic data to detect these geometry changes is assessed by performing synthetic seismic modelling of the production of a salt mine in the north of the Netherlands.

In the first section a brief overview of the geological history and the composition of the Zechstein formation in the north of the Netherlands is provided. How the specific magnesium salt minerals are mined is described next. Based on this knowledge four different scenarios describing the cavern growth in time are introduced. These scenarios are translated to seismic models and the seismic responses for each of them will be shown in the subsequent section. The main results in terms of observed time-lapse seismic differences will then be discussed. Finally, concise conclusions are given.

THE ZECHSTEIN MAGNESIUM SALTS: THEIR GEOLOGY AND MINING

History and composition of the Zechstein formation

The magnesium salts of interest in the north of the Netherlands were formed in the Zechstein era, the late Permian. At that time, the Netherlands was at the current position of the Sahara. The climate was a very humid and warm desert-like one, with high evaporation. A relative sea level rise created an enormous epeiric sea, called the Zechstein Sea. It covered what now includes the North Sea, lowland areas of Britain and the north European plain through Germany and Poland (see Fig. 1). The north of the Netherlands was on the border of this sea. The sea had only a very shallow connection to the Tethys Ocean. Water could only pour into this sea in the case of a relative sea level rise, whereas at low-level conditions the sea would retain an inflow of fresh seawater. During periods of relatively low sea levels, the evaporites were formed.

Many cycles of inflow of seawater and evaporation of salts have taken place. In the Zechstein formation in the north of the Netherlands, five main cycles are recognized, of which only the third contains magnesium salts. Many types of salt are found within the Zechstein formation, the relevant ones being

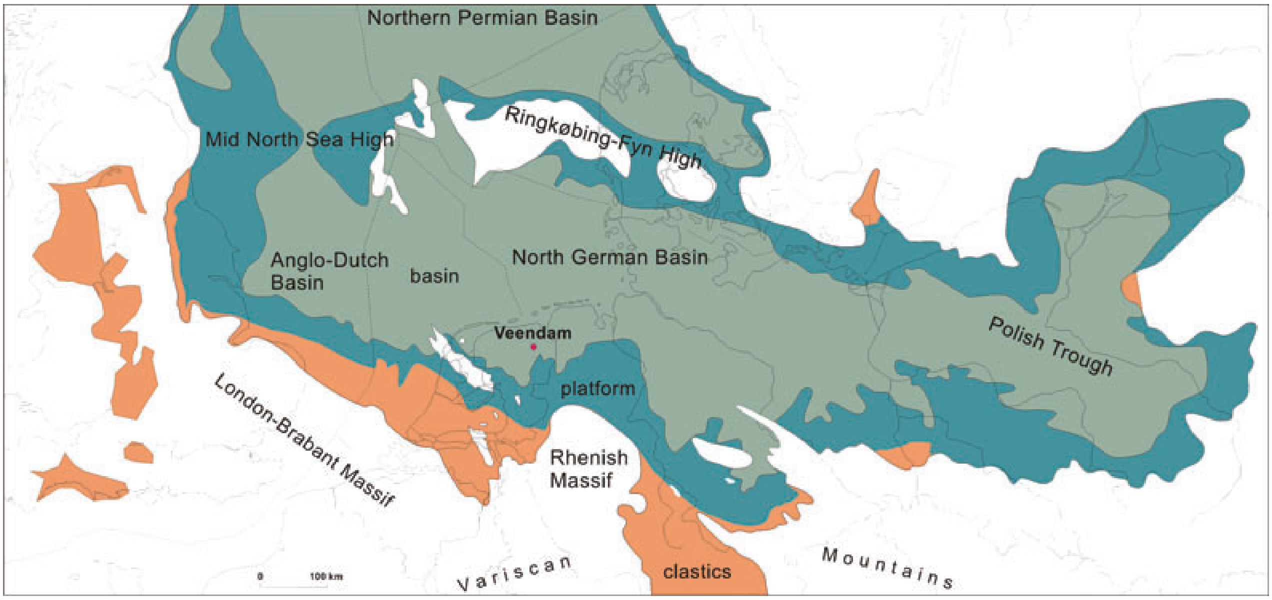

Figure 1 Present day distribution and facies map of the Zechstein Group in the Southern Permian Basin. Colours indicate different facies of the 2^{nd} evaporation cycle of the Zechstein (Z2) in which the salt was deposited: light green = basinal facies, dark green = platform facies, red = time-equivalent clastic deposits. Mine location at Veendam indicated (after Geluk 2005).

halite, kieserite, sylvite, carnallite and bischofite. Halite precipitates when 90% of the seawater has evaporated. Kieserite, sylvite, carnallite and bischofite precipitate from the remaining seawater.

Carnallite and bischofite are magnesium-salt minerals. Especially bischofite, which contains the highest amount of magnesium and therefore delivers very high-quality magnesium products, is very rare in the world. Carnallite is found in the whole of the northern Netherlands but bischofite is only found around Veendam, so it is most likely that this area was situated in a local depression, where all the not-yet-evaporated seawater was collected. It is hard to distinguish the different layers of the separate minerals and usually, a combination of them is found within one layer.

Mining history and methodology

During the discovery of the large Groningen gasfield in 1959, the thick Zechstein formation was drilled in the exploration phase. It was only then that the layers with a high content of carnallite and bischofite were discovered. Based on testing and further study, a first mine was installed near Veendam. The production of magnesium salt started in 1972. Nowadays, different types of magnesium and calcium products are produced, finding their way into a wide variety of applications. Table 1 provides an overview of the various magnesium salts with examples of their use.

Table 1 Products from carnallite and bischofite and examples of their use

Product	Examples of use
Magnesium oxide (MgO)	Cement and steel industry
Magnesium chloride ($MgCl_2$)	Textile finishing, catalyst production
Magnesium hydroxide ($Mg(OH)_2$)	Neutralizing acid waters
Calcium chloride ($CaCl_2$)	Dust control, road stabilization

The adopted method for mining especially carnallite until 1996 has been conventional solution mining (see Fig. 2a). Mining water is pumped down the well and the brine is pumped up through a separate inner tubing within the same well. The dissolution of the salts causes caverns to form. A note to make is that the exact shape of these caverns is not known.

In 1996 the method was changed to squeeze mining (see Fig. 2b). The focus shifted towards the bischofite that was not mined prior to that date. Squeeze mining is based on the phenomenon that magnesium salts become mobile under large pressure differences. The salts are pressurized by the overburden and the caverns are kept at a relatively low pressure of 65 bar, which is below the lithostatic pressure. This pressure difference causes the salts to creep towards zones of lower

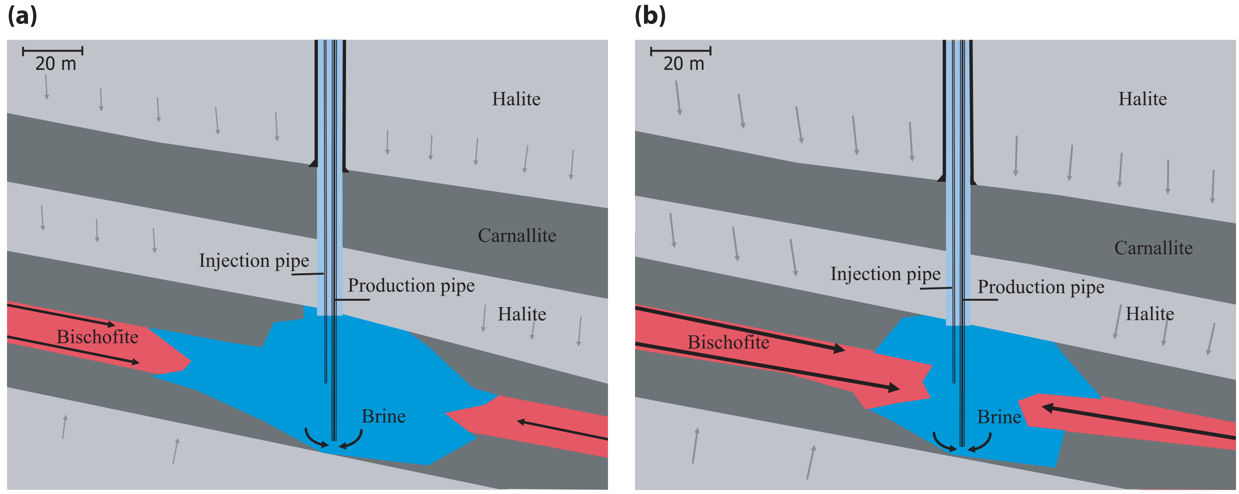

Figure 2 Migration to the caverns. The higher the difference, the quicker migration takes place into the cavern. a) When the pressure in the cavern equals the rock pressure, no mass transport occurs and the salt is only dissolved by the injected water. b) The explanation for squeeze mining is that mobility of the different salts depends on the different materials (roughly 1:10:100 for rock salt: carnallite: bischofite). Due to pressure difference between the cavern and the rock, salt tends to migrate towards the cavern. This implies that caverns remain relatively small during leaching.

pressure. Although the degree of creep is not well understood, it has been established that halite shows a much lower creep than carnallite, which in turn shows a much lower creep than bischofite. Although the strain rate depends on differential stress, the strain rates can be estimated very roughly, in order of magnitude, as 1:10:100, respectively (Urai *et al*. 2008, Fig. 5.2.). The bischofite will therefore creep towards the caverns, resulting in a gradual thinning of the salt layer. Bischofite will creep due to pressure difference between lithostatic pressure depending on the depth and the pressure applied in the cavern.

For the development of cavities it is important to note that squeeze mining has a different effect than conventional mining under lithostatic conditions, because part of the created brine is replaced by solid salt. This enables production of more salt from the same cavern.

A counter-effect is that squeeze mining leads to a more rapid surface subsidence than conventional lithostatic mining, in which there is no net volume change in the salt layers. The squeeze mining leads to extra deformation of the overburden, which in turn causes extra subsidence of the Earth's surface. Dutch regulations now impose a maximum subsidence of the surface of 65 cm for this mine, limiting production in the future. This demands an optimized strategy. In order to improve current predictive modelling of the process and to optimize the process, more knowledge is required on the geometry of the developing cavern. The purpose of this study is to investigate whether time-lapse seismic data can provide the necessary constraints on the geometry of the cavern development.

DEFINITION OF SCENARIOS FOR SALT PRODUCTION (SQUEEZE MINING)

As mentioned in the introduction, the goals of this study can be summarized as follows: can the effects of solution salt mining be observed and quantified in seismic time-lapse mode? and can the geometry of the brine cavern developing in time be detected by time-lapse seismic imaging? The setting is quite different from 'conventional' applications such as hydrocarbon production or CO_2 storage in the sense that:

- the volumes of salt production are much lower than the fluid production/storage in 'conventional' time-lapse applications and
- the solids are essentially replaced by fluids in the salt application, giving much higher and other impedance-contrast changes than in 'conventional' time-lapse applications.

In order to address these questions, different production scenarios have been defined that capture the different possibilities of the salt production as described in the previous section and then specifically focused on the current mining method, squeeze mining. Note that for conventional solution mining the geometry of the scenario (i.e., the cavern filled with brine) would not change, only the amounts of salt production per year. The presented scenario is fully dimensioned on squeeze mining production rates. The only quantitative

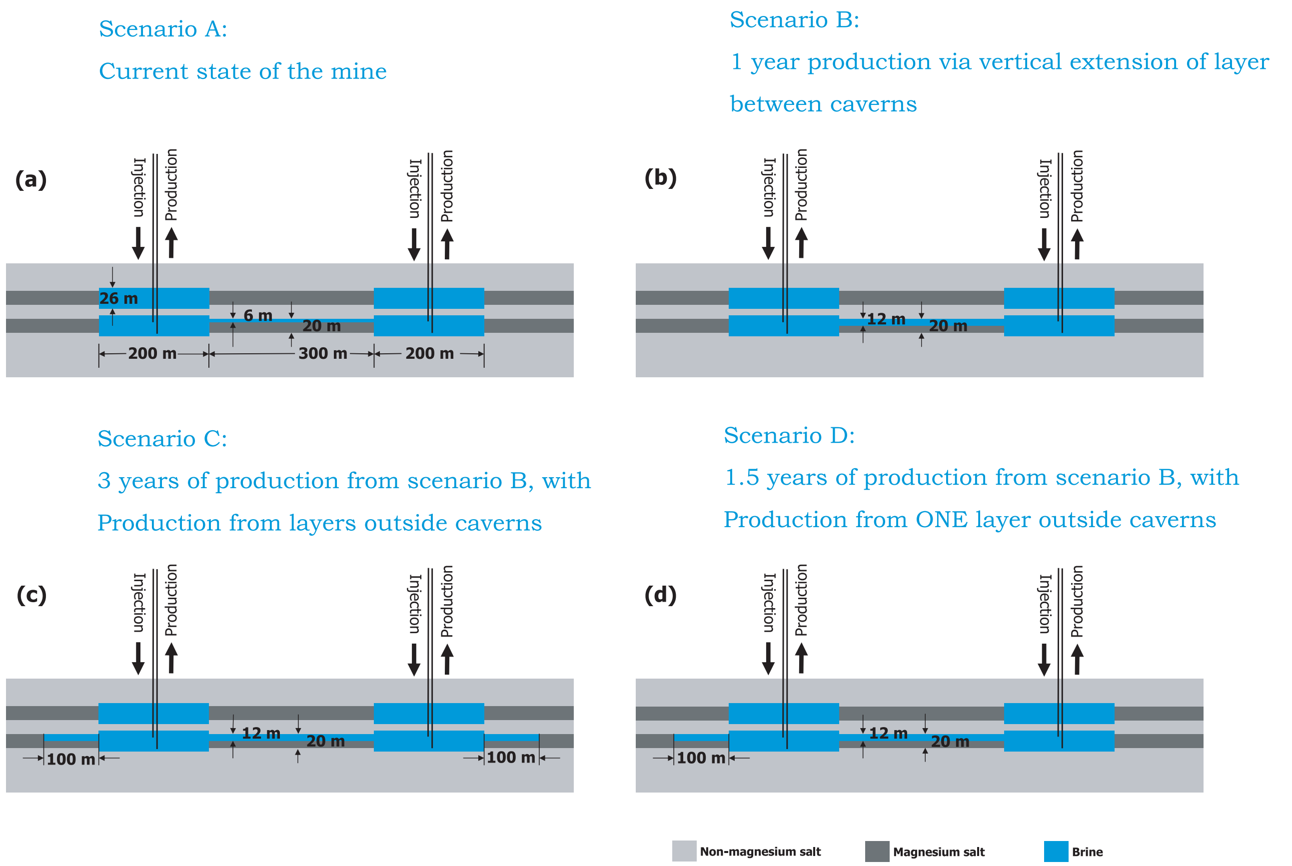

Figure 3 Schematic views of scenarios A–D, for production from the lower magnesium-salt layer. a) Scenario A: current state of the mine. b) Scenario B: 1 year production between caverns. c) Scenario C: 3 years production from outside caverns. d) Scenario D: 1.5 years production only from the left-hand side of the left-hand cavern.

information available is the volume of produced salt, being on average some 27 500 m^3 of salt per year per well. This number has been used as a constraint in the scenarios.

Currently, magnesium salt is only mined from the lower of two magnesium salt layers. Pressure measurements in different wells indicate lateral communication of the brine in the lower layer. In the scenarios this has been taken into account by introducing a brine connection as a layer of constant thickness at the top of the lower magnesium layer. In time, different thicknesses are assumed in the scenarios, interpreted as a 'vertical' production of the salt. The laterally-oriented production of the salt is assumed to be caused purely by magnesium salt squeezed towards the caverns from the magnesium salt layer outside the caverns.

In total, four scenarios have been defined, starting from the 'best guess' of the current situation. Schematically, they are shown in Fig. 3. Figure 3(a) represents the current state of the mine. There are two caverns at every well, where the caverns are modelled in 2D as rectangles. Between the caverns there is the producing salt layer. For scenario B, as shown in Fig. 3(b), it is assumed that during a year of production the magnesium salt layer has been replaced by brine for six more metres in the vertical direction between the two main caverns.

Scenario C is then the purely lateral effect based on the real salt production of 27 500 m^3 per year per well and a height of 12 m. This is shown in Fig. 3(c). This corresponds to a production of three years after scenario B, or four years after scenario A. Finally we have included a less likely scenario D (Fig. 3d) in which production only takes place on one side. The aim of scenario D is to investigate whether asymmetrical production will show up.

PARAMETRIZATION OF THE SEISMIC MODEL

The next step is to convert these four scenarios into model parameters required for seismic modelling, i.e., the P- and S-wave velocities and the mass density. In this section, we will

Table 2 Initial P-wave velocities ($c_{P,0}$), velocity-gradient (k) and mass-density (ρ) values for different era or rock types

Era/Rock	$C_{P,0}$ [m/s]	k [1/s]	ρ [kg/m^3]
Cenozoicum	1750	0.32	2000
Cretaceous and Jura	2500	0.86	2600
Trias	2900	0.37	2700
Gypsum and halite	4600	0	2170
Carnallite and bischofite	4300	0	1600

briefly explain how we obtained these parameters and their distribution around the mine. Note that for computational reasons only, variations in 2D have been considered.

P-wave velocities

For the P-wave velocity the Velmod-1 model as given in Dalfsen *et al.* (2006) is used. It is based on information gathered from 720 wells in the Netherlands. Via a least-squares procedure, parameters for velocities (c_P) as a linear function of depth (z) of the form $c_P = c_{P,0} + kz$ were found for the different era; $c_{P,0}$ is the velocity at the surface ($z = 0$). In the table below (see Table 2) the values are given. The Velmod-1 model does not provide information on the velocities within the Zechstein formation, while for our work it is obviously the most important one. For the Zechstein formation the velocities are derived from sonic logs from wells of the mine, obtained in the 1970s. The average values for each formation are given in Table 2. For the mine, the caverns are filled with brine. The P-wave velocity of the brine is probably slightly higher than of water because of the dissolved salts and the higher pressure. However, since no measurements are available and the effect is estimated to be minor, a constant water velocity of 1500 m/s has been assumed irrespective of the dissolved salt content.

S-wave velocities

No measurements have been taken in the boreholes of the mine to determine the shear-wave velocity. In order to create a S-wave velocity model, Castagna's empirical relation for saturated sandstones (Castagna, Batzle and Eastwood 1985) has been used for formations other than the Zechstein salts:

$$c_s = 0.804 c_p - 856\,(m/s)\,. \tag{1}$$

For the Zechstein formation, the shear-wave velocities were obtained by assuming a Poisson's ratio of 0.35 for all types of salt as suggested by Jeremic (1994). For the mine, it is assumed that the caverns filled up with brine have a shear-wave velocity of 0 m/s.

Mass densities

The mass densities are derived from density logs. The original logs and their interpretation from the mine archives were used. A single density value is assigned to each layer (Table 2). For the brine in the mine, an accurate density measurement exists of 1.335 kg/m^3.

Structure of the model

The structure of the model is based on real 3D seismic data obtained in 1992, as part of the hydrocarbon exploration. These data show the salt mine. A 2D section out of the 3D data crossing the mine is shown in Fig. 4. The mine is clearly visible indicated in the figure by a black rectangle.

Based on these data, the main formations were picked to define the structure of the model. Only the total P-wave velocity model for the current situation (scenario A) is plotted in Fig. 5 but the S-wave-velocity and mass-density model follow the same structure.

MODELLING THE SEISMIC RESPONSES AND PROCESSING THE DATA

The next step is the seismic modelling. Here we used an elastic (lossless) 2D finite-difference scheme, as described in Virieux (1986). In our scheme, a 4th-order scheme in space and 2nd-order scheme in time is used, taking a staggered and explicit grid.

The first model made is a 2D model referred to as the base model (scenario A), which describes the current situation so including the salt mine in its present form. The full model is 17 km wide (x-direction) by 4.5 km deep (z-direction), divided into grid blocks of 2 m $\times$ 2 m. The centre of the mine is at 13.55 km in this model. The model is extended such that artificial reflections from the sides of the model do not interfere with the reflections around the mine. A total of 144 shots were generated, with a source spacing of 48 m and a receiver spacing of 24 m. The time sampling was 4 ms. As a wavelet we used a Ricker wavelet, a second-derivative Gaussian, with a peak frequency of 15 Hz. With these parameters, the calculation times were some 20 hours per shot and, in order to do the calculations in a reasonable time, a cluster of 26 computer nodes was used.

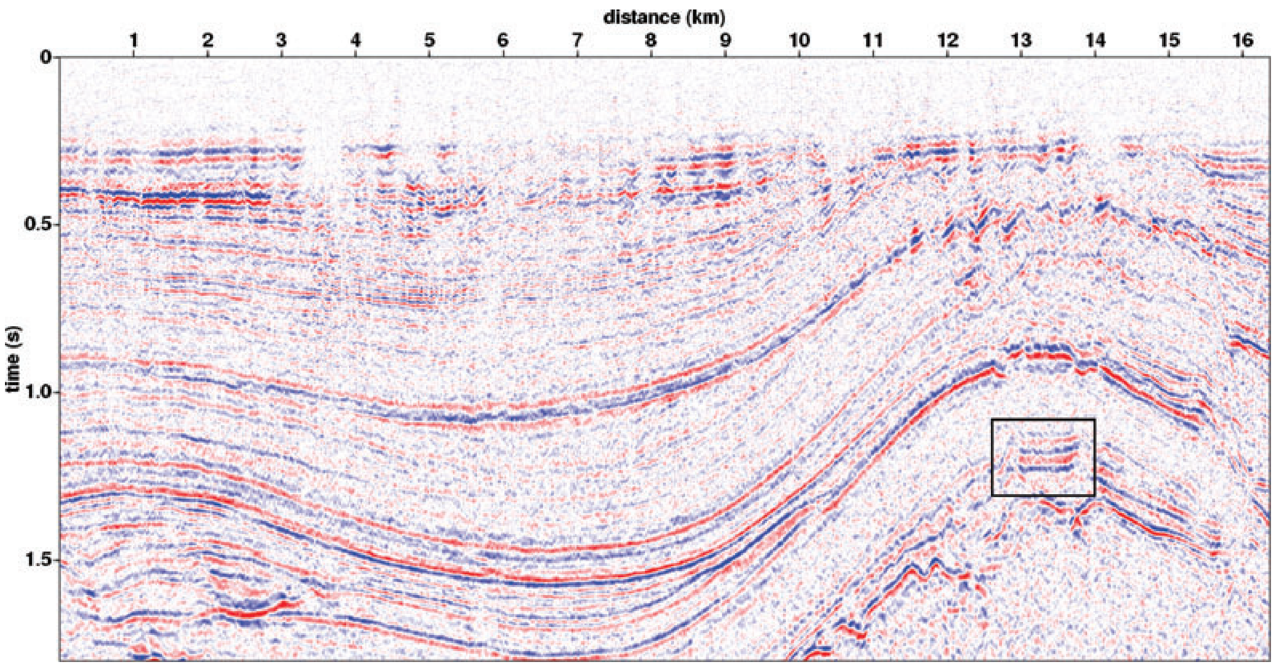

Figure 4 Seismic section through the salt mine. Data taken from a 3D data set from Nederlandse Aardolie Maatschappij (NAM) in 1992. Rectangle indicates the location of the mine.

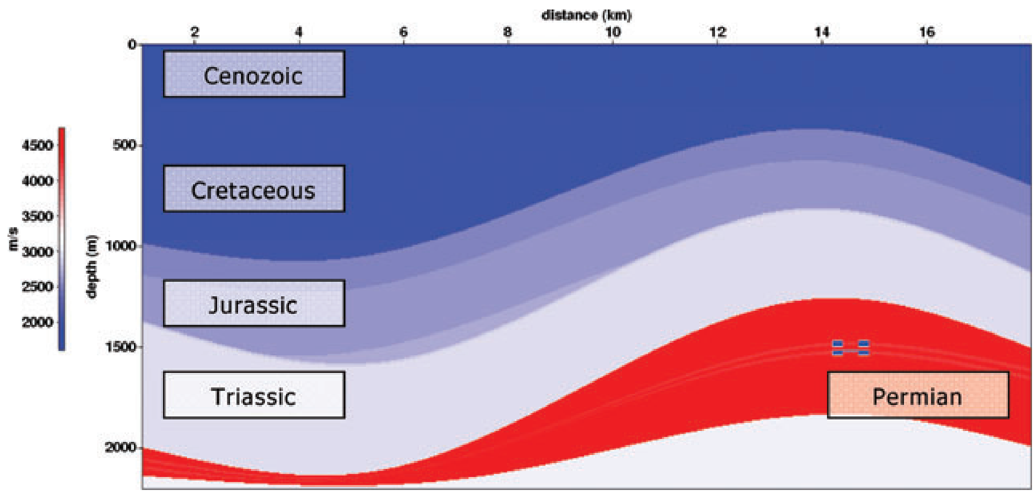

Figure 5 P-wave velocity model for scenario A.

A typical shot record is shown in Fig. 6. The shot is positioned at $x = 13.3$ km, located exactly above the left cavern of the salt mine. All the relevant events are indicated in the figure. A reflection of the mine is very clearly visible and indicated.

Processing

The goal of the modelling is to look at possible time and amplitude changes in the seismic data for the different scenarios. This entails processing of the data. The main processing steps for obtaining final images are: removal of the direct waves, prestack time migration and stacking. A prestack time migration based on a smooth background model was chosen since also in the real-data case the velocity model is not accurately known, especially within the salt. As an algorithm a Kirchhoff migration was used. The needed traveltimes are obtained from ray tracing through the root-mean-square (RMS) velocity model. The RMS-velocity model was based on the model

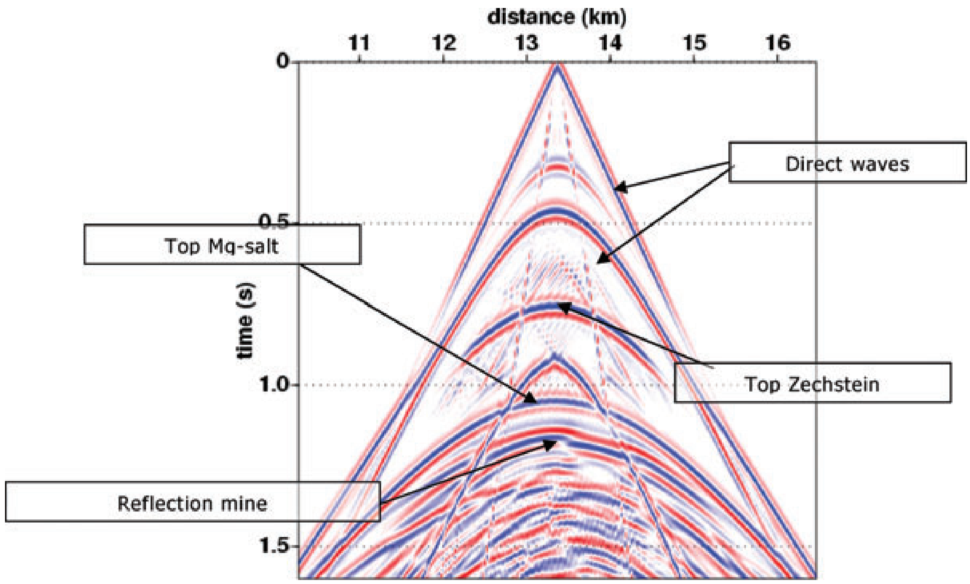

Figure 6 Record for a shot at $x = 13.3$ km, right above the salt mine, of scenario A.

without the mine and obtained from direct conversion from the interval velocities as given in the previous section. This model was used for all the scenarios. The error introduced because of the mine and their production changes was estimated too small to have a significant effect on the migration results.

Final imaging results

The stacked time-migrated section through the salt mine for scenario A is shown in Fig. 7. The reflection of the mine comes forward as a very clear bright spot, caused by the large impedance differences. The reflection also gives an idea about the geometry of the salt mine; it shows the two caverns at the sides and the layer between the caverns. The resolution is limited in seeing all the exact details of the mine, such as the separate caverns on top of each other but it should be kept in mind that with a peak frequency of 15 Hz and RMS-velocities of some 2000 m/s around the mine, the dominant wavelength is around 133 m, a size comparable to the sizes of the caverns of the mine and a size much larger than the thickness of the magnesium-salt layer from which the salt is produced.

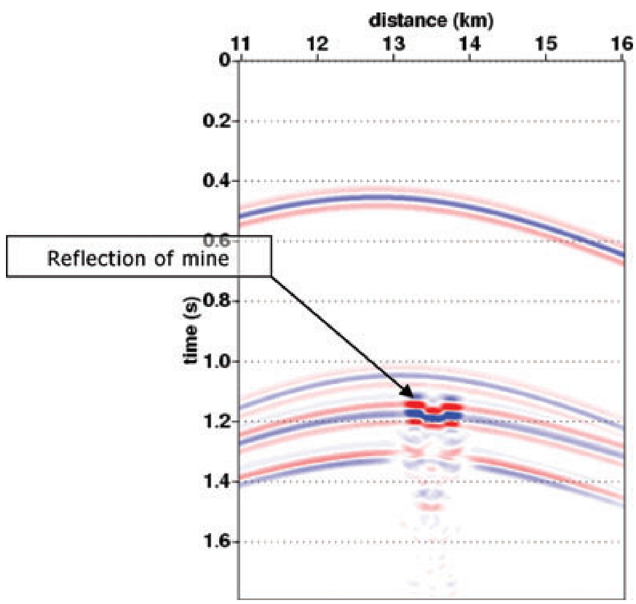

Figure 7 Prestack time-migrated reflectivity image of scenario A, with a reflection of the salt mine indicated.

PRE-IMAGING TIME-LAPSE EFFECTS DUE TO VERTICAL AND LATERAL CHANGES OF THE MINE

In this section it is shown how vertical and lateral changes of the brine affect the time-lapse responses in the pre-imaging stage, since stacking and time-migration average and smooth the signal. We will have a look at snapshots and zero-offset data and their sensitivity to changes in the mine, before looking at full-offset CMP (common-midpoint) data. First, we will briefly introduce the two analysis techniques employed.

Analysis methods: differencing

A difference data set allows a good visualization whether differences exist. Differencing is very sensitive to time-shifts. It very much highlights where changes are taking place in the subsurface and therefore is most suitable for detection purposes. However, it should be realized that a difference section does not give the time-shift and/or amplitude change itself. Via modelling the effect, an accurate estimate of the time-shift can be made. Based on the subtraction of the two data sets, the well-known NRMS attribute (Kragh and Christie 2002) can be determined.

Analysis methods: 1D cross-correlation

In this paper cross-correlation in the vertical direction, as commonly done in time-lapse analysis, is used for the quantitative determination of the full-waveform changes. From these waveform changes attributes like time-shifts and amplitude changes can be extracted. In the vertical direction, time-shifts are usually a fraction of the original time sampling of most seismic data sets (2 or 4 ms), so therefore the data need to be interpolated in time. For the extraction of the waveform attributes, a time window around the area of interest is taken and the interpolation is then taken care of by adding zeroes in the Fourier domain.

Snapshots

Before starting to quantify the changes, we first have a look at differences in the wavefields at one time in the space domain, i.e., snapshots. Based on snapshots, an impression can be given of the type of differences that can be expected. To this end, the snapshots in Fig. 8 are shown: a vertical (scenario B–A) and lateral production (scenario D–B) of the mine for a shot right above the mine, at two different times; and these two

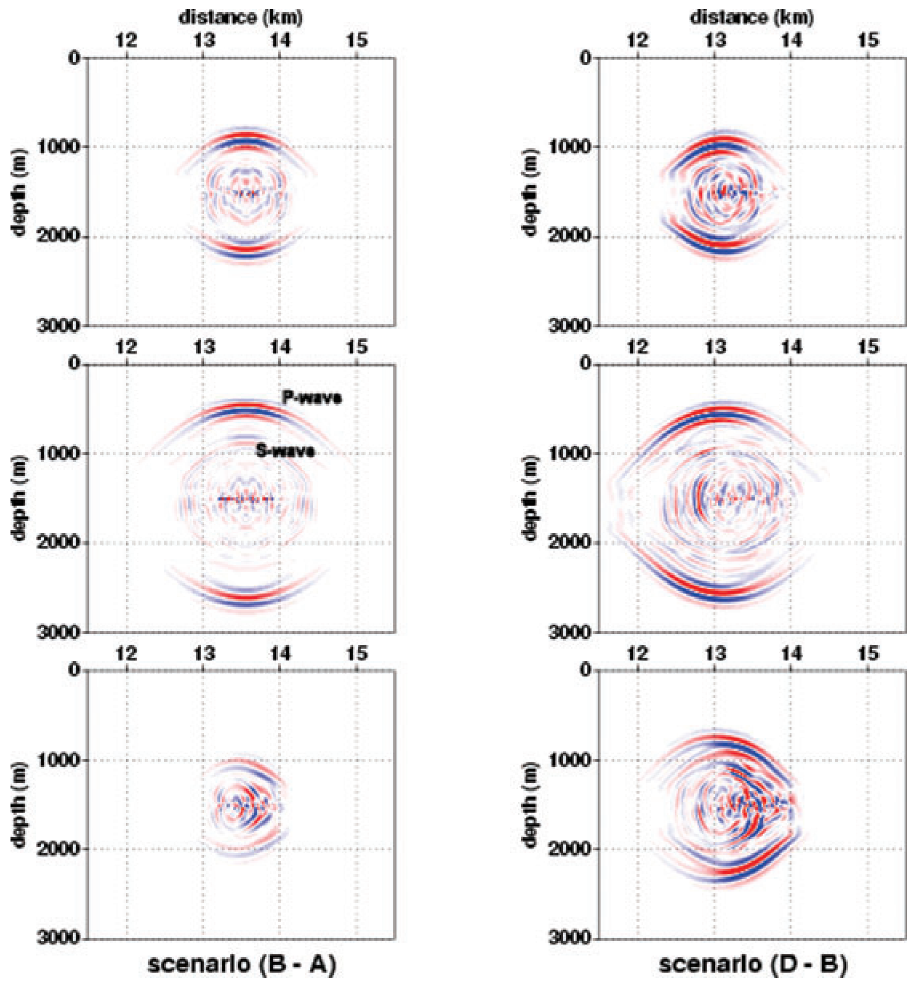

Figure 8 Snapshots of differences of wavefields for different production scenarios. Left column: vertical production (difference between scenario A and B). Right column: lateral production (difference between scenario B and D). Top and middle: shot right above the mine ($x = 13\ 355$ km), for times 0.875 s (top) and 1.025 s (middle). Bottom: offset shot left of the mine ($x = 11\ 976$ km) at time 1.025 s.

production scenarios for an offset shot, some 1.5 km to the left of the mine but then only once.

The first main observation from all the snapshots in Fig. 8 is that the difference wavefields seem to occur from localized 'points', consistent with the production of the mine being small or comparable to the wavelengths. Another observation that can be done is that the snapshots show a first/outer P-wave 'difference diffraction' but also a second S-wave 'difference diffraction', showing the elastic character of the difference wavefields. Looking at the snapshots for the shot right above the mine, it can be observed that for the vertical production of the mine a symmetrically-shaped difference wavefield is generated, while for the lateral production of the mine the difference wavefield is somewhat skewed and the amplitudes are also differently distributed. At the bottom of the figure snapshots are shown for the offset shot. Here too significant differences can be seen in shapes, amplitudes and arrival times for the two production scenarios.

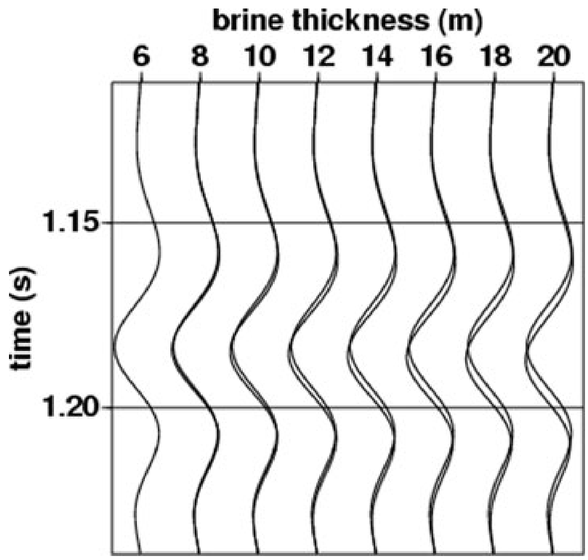

Figure 9 Zero-offset traces in the middle above the mine for different thicknesses of the brine layer. For comparison purposes, the reflection for the 6 m thickness has been plotted on the top of each response, giving an impression of the time-shifts and amplitude changes to be expected.

Zero-offset data above the mine for vertical changes of the mine

In order to quantify the changes in the seismic signal due to vertical changes of the mine, a range of brine thicknesses was modelled. This was done on top of the modelling for the scenarios defined earlier but only one shot for each situation was needed now since no full imaging is done. The reference state for the vertical extension has a brine thickness of 6 m, while for the production stages higher thicknesses were taken up to 20 m in steps of 2 m. One shot centrally positioned above the mine was modelled for all the states. From these shots, the zero-offset traces were taken and a time window around the reflection of the mine chosen. In Fig. 9 the waveforms for the different brine thicknesses are given, to show the full changes taking place.

Based on these traces, the 1D cross-correlations were performed and the time-shifts and amplitude changes extracted. The peak values of the cross- correlation were scaled by the peak values of the autocorrelation of the reference state of 6m to obtain the amplitude changes. The time-shifts and amplitude changes are shown in Fig. 10. As can be seen in this figure, the time-shifts increase linearly with an increasing vertical extent of the brine layer. The difference between 12 m thickness and 6 m thickness, the difference between scenarios B and A, leads to a time-shift of some 1.75 ms. The linear trend is about 0.23 ms/m. The amplitude change is not a linear function of the vertical extent and there is an interference effect. The maximum change is about 6.6%, occurring around scenario B, i.e., a brine-layer thickness of 12 m. Beyond this the amplitude change decreases and can become even negative beyond 20 m thickness.

Common-midpoint data

In the above, good first quantitative indications of the time-shifts and amplitude changes are given. However, these data were only zero-offset data, located in the middle above the mine. Now the differences of full-offset common-midpoint (CMP) data are considered. We also consider the lateral differences by comparing CMPs to other CMPs. This is important since the mine is not one but two caverns and we have different producing parts of the bischofite layers between and away from the caverns. It will be seen that the changes not only happen at the dominant reflection but also at later times, being caused by different parts of the mine. As for the shot as previously shown in Figure 6, the reflection of the mine is prominently present in the CMPs for all scenarios, especially for the CMPs above the salt mine.

Let us now look at differences in the CMPs, as shown in Fig. 11. In this figure the results are shown that are directly related to the vertical (from scenario A to B) or horizontal production (from scenario B to C or D) of the mine. CMPs are shown located above the left cavern (left column of Fig. 11),

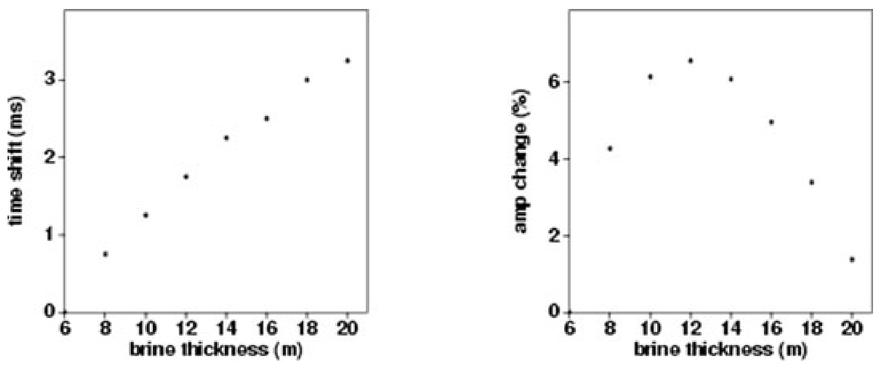

Figure 10 Time-shifts and amplitude change as a function of brine layer thickness. Changes compared to the reference state with a brine thickness of 6 m.

above the producing layer between the caverns (middle column of Fig. 11) and above the right cavern (right column of Fig. 11). So differences between the different scenarios are shown in the different columns of Fig. 11. For the rows in Fig. 11, each row is scaled by the same constant, in this case by the maximum amplitude of the left CMP. So then differences between different spots above the mine can be compared, also amplitude-wise.

The top row shows the differences between scenario A and B so a production of 6 m in the layer between the caverns. The largest change, amplitude-wise, is seen in the CMP in the middle. Also this CMP shows the differences earliest. Both these observations are as expected since the middle CMP is located above the producing layer.

On the next row the differences are shown for lateral extensions of the mine in two directions. It can be seen from the two outer CMPs that two difference-events can be seen, the later one being due to the production of the extension on the other side. As expected, the first 'event' is earlier than in the middle CMP, since the left and right CMPs are above the extensions themselves. For the interpretation of the middle row, the bottom row helps too since the bottom row represents a production from one side. From the bottom row it is clear what the effect of one extension of the mine is: the CMP above the extension shows the earliest difference and is also largest in amplitude.

TIME-LAPSE EFFECTS AFTER IMAGING

In this section we will focus on the stacked time-migrated images and the effects of the different scenarios for the salt production. Zoomed-in sections for the current situation and the three production scenarios are given in Fig. 12. It can be observed that the extension of the brine layer in the vertical direction leads to an increase in amplitude and a little sag of the reflection in the middle. It can also be observed that the migrated sections of scenarios B and C look pretty similar but the reflection in scenario C is more extended and lower than the cavern, which is caused by the extension of the mine in the lateral direction. The figure gives a good idea of where the changes of the mine have taken place, in a qualitative manner.

Next, the changes of the images as depicted above are analysed in a quantitative manner. Here, the imaged sections are subtracted and cross-correlated, the first for detection and window selection, the second for quantification. The time-shifts and amplitude changes found by the cross-correlations of the different scenarios are discussed. The changes are determined by sub-sampling the data-window with a factor 16 for the time-sampling, i.e., from 4 to 0.25 ms.

Let us first consider the differences in the imaged sections. We again take the same different scenarios as we took for the CMPs. They are shown in Fig. 13. From these images it is very clear where the changes are taking place. On the left-hand image a vertical production from the layer between the caverns is very obvious; in the middle image the production from the layer outside the caverns can be directly observed; and in the last image on the right, the production from the left-hand side is obvious.

In order to quantify the time-shifts and amplitude changes per lateral position, 1D cross-correlation is performed. For the three most characteristic changes from the three production scenarios, this is shown in Fig. 14. In this figure, it can first be observed that the largest correlation is around time zero, which is due to the fact that the images themselves have the highest amplitude there. Looking at these main lobes, it can be observed that there are some time-shifts involved and,

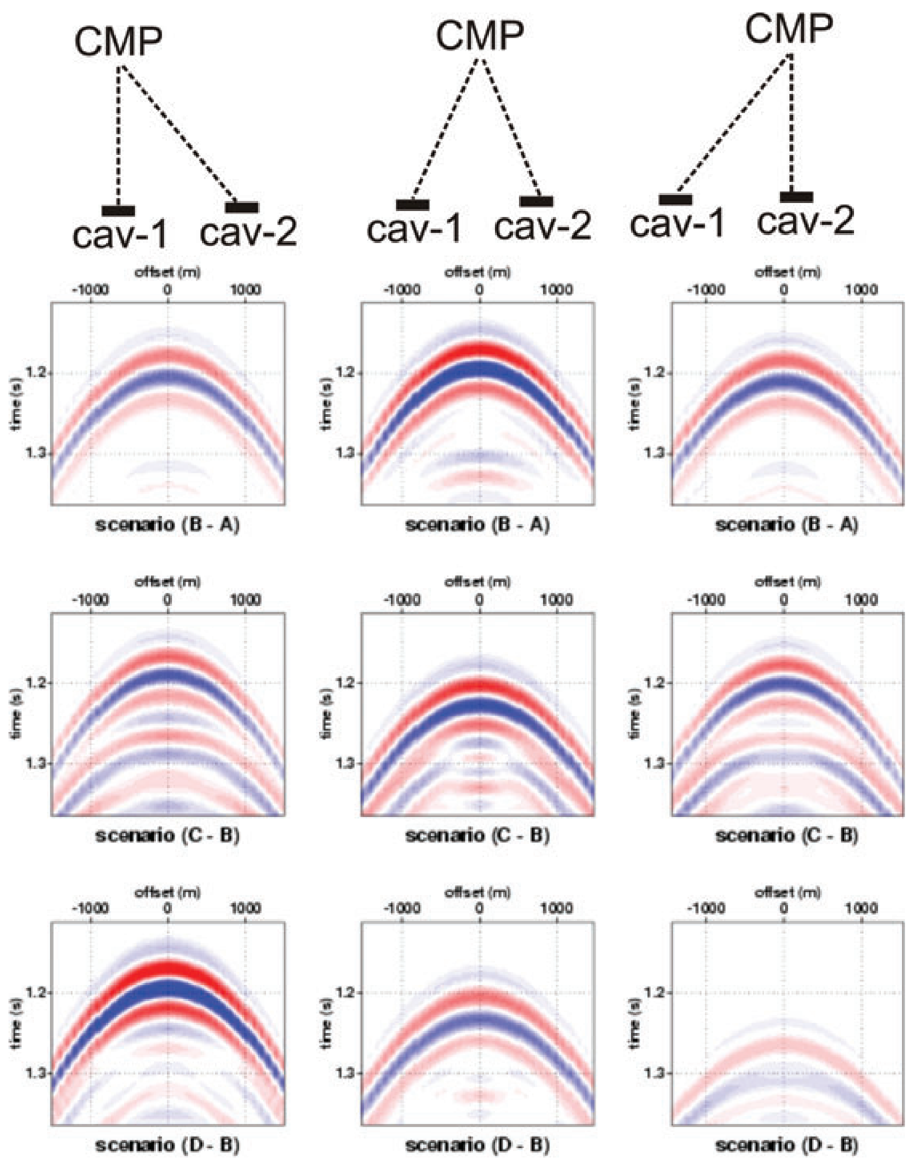

Figure 11 Differences between CMP's for different production scenarios. As indicated by sketches on the top: left column = CMP1 at 13 296 km, middle column = CMP2 at 13 548 km, right column = CMP3 at 13 800 km. Top row: difference between scenarios A and B. Middle row: difference between scenarios B and C. Bottom row: difference between scenarios B and D.

although not so obvious from the cross-correlation images, amplitude changes also occur.

Next, let us look at the time-shifts and amplitudes extracted from these correlations. They are given in Fig. 15. The leftmost plots can be compared to the zero-offset results shown earlier (Fig. 10). Here the changes are slightly different due to the time migration and stacking. Here, time-shifts of some 4 ms can be observed in the middle, above the mine, for production in the vertical direction of the mine, which is a bit higher than in the pre-imaging zero-offset trace. The amplitude change is variable with some maximum above 20%. This is significantly higher than in the pre-imaging zero-offset trace.

Next, let us consider the lateral production, as given in the other plots of Fig. 15. Both in the time-shifts and amplitude changes, high values are obtained in the areas where changes take place. These are high values since in the reference scenario B there is no brine in the magnesium-salt layers outside the caverns, while in scenarios C and D there is. Therefore, changes are very obvious but quantification of these changes does not add much extra information.

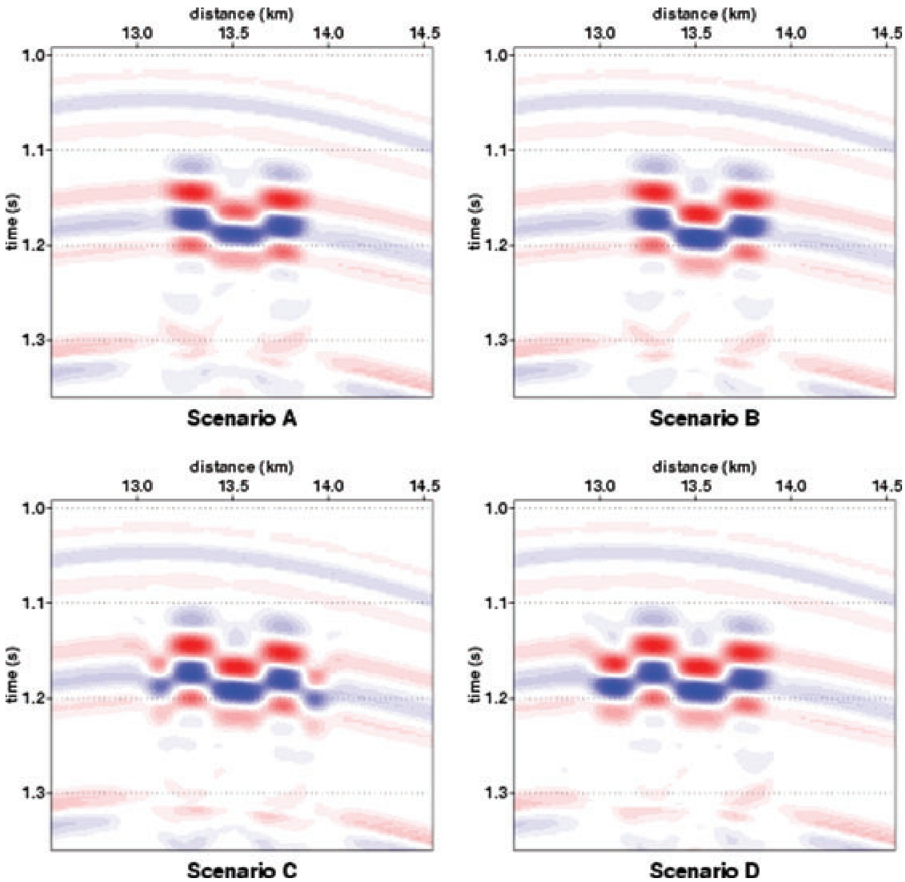

Figure 12 Sections zoomed-in on the reflection of the salt mine for production scenarios A to D. All plots are scaled with one common amplitude.

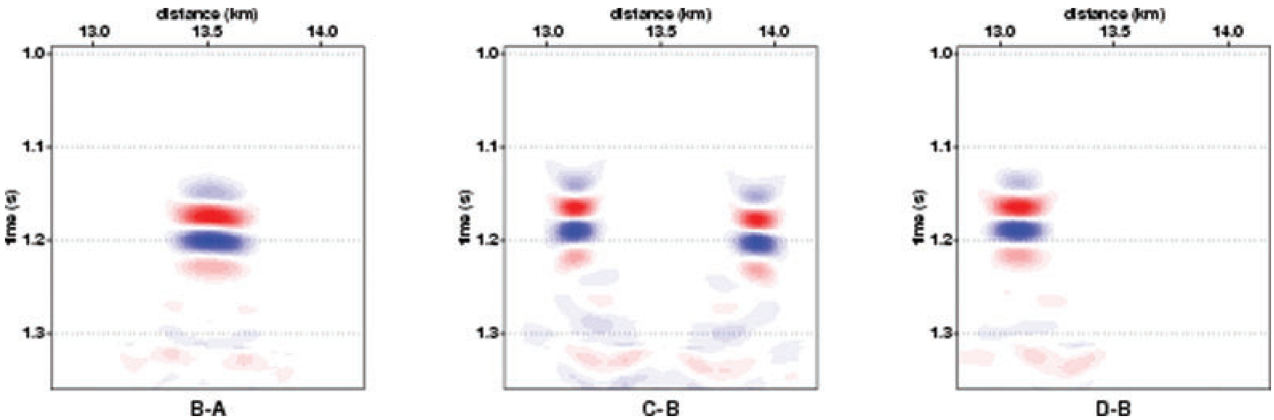

Figure 13 Differences of imaged sections for different production scenarios. Left: between scenarios A and B. Middle: between scenarios B and C. Right: difference between scenarios B and D.

DISCUSSION

In the above it is shown quite convincingly that time-lapse seismic techniques can be employed to monitor salt production from solution salt mining. As a first result this is very good but not all issues have been taken into account, like the issues not captured by the assumptions in the modelling.

One issue is the issue of noise, especially when monitoring on land, being surface-related and often related to the shear-wave properties of the near-surface. One source of noise is

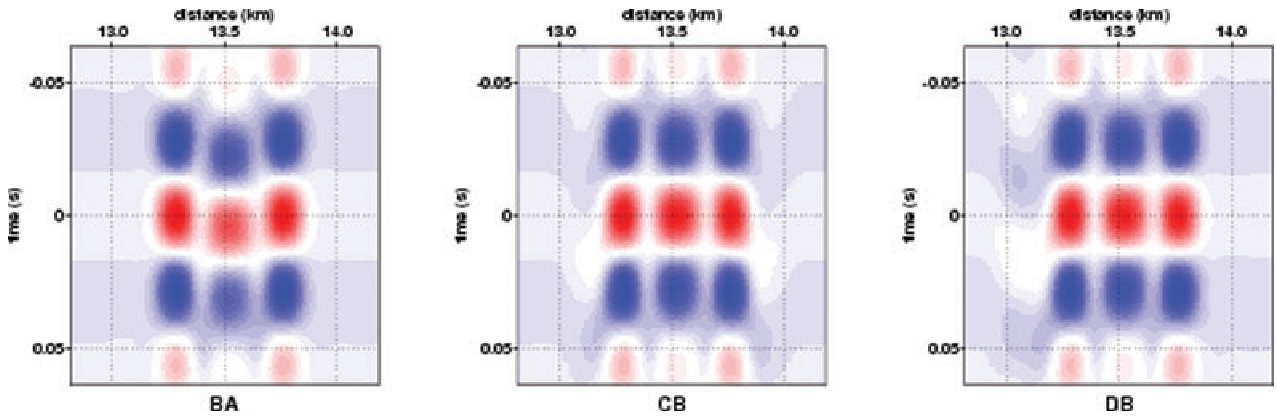

Figure 14 1D cross-correlations between imaged sections for different production scenarios. Left: between scenarios B and A. Middle: between scenarios C and B. Right: between scenarios D and B.

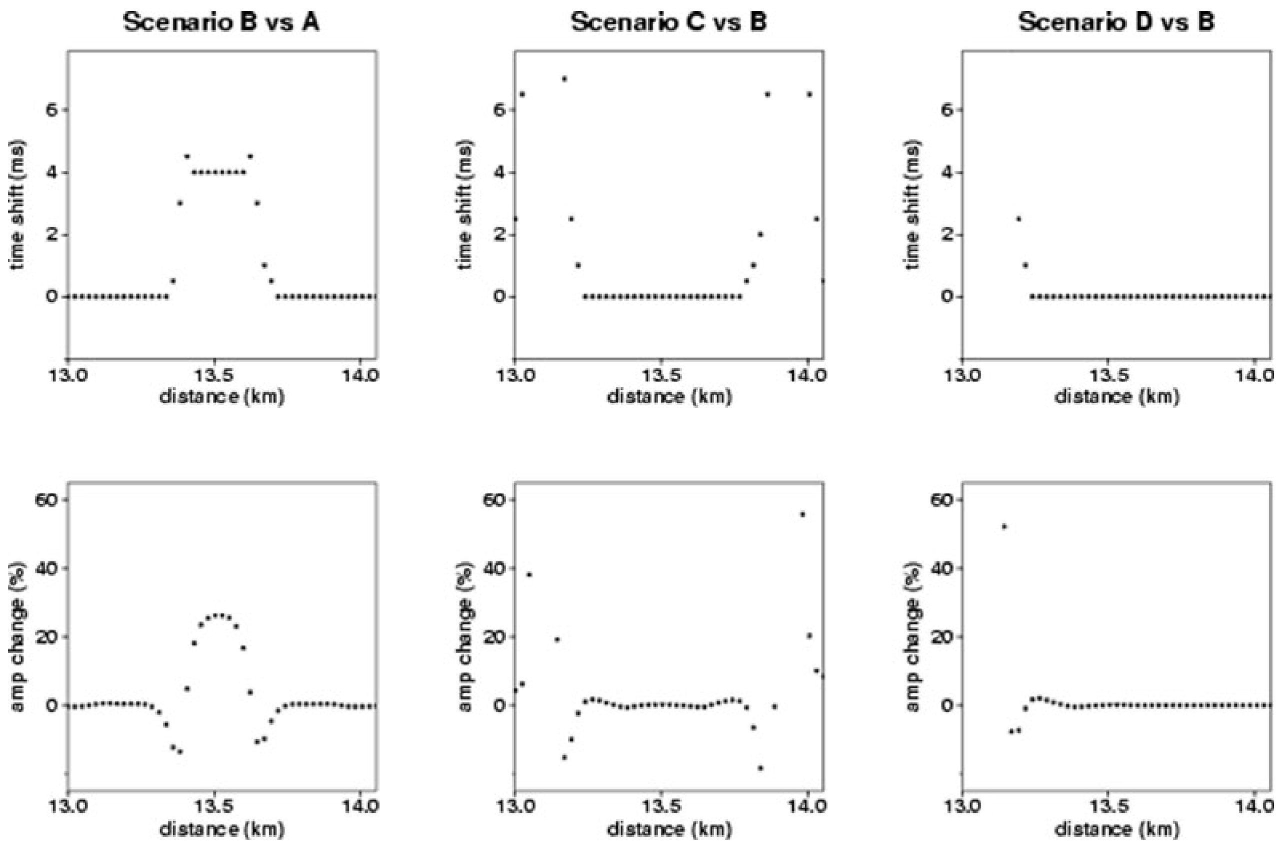

Figure 15 Time-shifts and amplitude changes due to different production scenarios.

the noise level. Real-field noise levels should be taken into account to show that the changes observed in the synthetic data are observable well above these levels. It could well be that on land, permanent buried stations are necessary or at least, desirable. It has been shown that surface-related noise is decreased significantly when burying the receivers (Drijkoningen *et al*. 2006), being a better noise suppressor than a dense array of receivers at the surface. It has also been shown that repeatability increases when stations are buried (Schissele *et al*. 2009).

Another source of noise is related to the spatial wavefield sampling for monitoring. In this study we made a choice for sufficient wavefield sampling for imaging purposes, ignoring the requirement for sufficient spatial sampling for noise suppression. Usually on land and thus also for monitoring, the noise suppression requires a (much) denser sampling than the imaging, the noise being due mainly to surface waves but to a lesser extent also to (shallow) shear waves. To make proper choices, knowledge of the characteristics of the noise at the particular study area is required, which often needs some real (noise-spread) data. We did not model and/or take this into account and therefore, optimal acquisition geometry for the real case has not been investigated.

Another issue is the overburden effect. In the discussion on the mining methodology, surface subsidence has already been mentioned, since it is currently occurring. This means that there is an overburden effect, next to the effects of production at the mine itself. There are some geomechanical effects of the overburden that may need to be taken into account in the seismic processing and analysis, affecting the imaging of the subsurface via velocity changes, due to stress changes and minor structural changes (Hatchell and Bourne 2005; Angelov 2009).

The last issue worth mentioning is the inversion issue. It has been shown here that geometry changes in the vertical and lateral directions and gives different time-shifts and amplitude changes. The results here look to be suitable for inversion but the expected horizontal and vertical resolutions are such that it would not be easy to obtain a very detailed map and change-map of the mine itself. Improved field conditions, such as permanent buried sources and receivers, may be required to increase the frequency contents of the data and therefore, the resolution of the results.

CONCLUSIONS

In order to better understand the effects of salt production, a feasibility study was performed to investigate its effects on the changes in seismic responses, i.e., in seismic time-lapse mode. The salt mine studied here, the magnesium-salt mine in the north of the Netherlands, is well visible in the seismic data. More importantly, changes for different production scenarios are also well visible as changes, both in the pre-imaging and the post-imaging data.

In order to quantify the changes, the full responses/waveforms around the reflection of the mine are correlated and from these correlation panels time-shifts and amplitude changes are extracted. The analysis on pre-imaging data shows that a vertical extension from 6–12 m of the magnesium-salt layer in the middle of the mine causes a time-shift of the order of 2 ms and an increase of some 6% in amplitude. From 6–20 m of production, the time-shifts change linearly with production while the amplitudes show a non-linear behaviour, initially increasing but after 12 m of production starting to decrease. In differences of CMP panels both significant time-shifts and amplitude changes can be observed at different locations above the mine, showing the separate 'difference' events due to the production at different parts of the mine.

The analysis on post-imaging (prestack time-migrated and stacked) data also reveals very significant changes in the seismic data. For vertical production, time-shifts of ~4 ms and amplitude changes of 20% or more are obtained. These values are as large if not larger than the ones obtained in the oil and gas industry. For a purely lateral extension of one or two sides of the caverns the changes are large due to the fact that the correlation is made with a situation when there is no brine layer, i.e., only a weak reflection. In these cases it even becomes more obvious where changes are taking place.

The conclusion therefore yields that the effects of solution salt mining on time-lapse seismic can definitely be seen and quantified with time-lapse seismic techniques and it therefore seems feasible to use time-lapse seismic to monitor the changes in and around the solution salt mine. Moreover, the effects are large enough that observable time-lapse effects are also to be expected in real seismic data.

REFERENCES

Angelov P.V. 2009. *4D seismic reservoir characterization, integrated with geo-mechanical modeling*. PhD thesis, Delft University of Technology.

Arts R., Eiken O., Chadwick A., Zweigel P., van der Meer L. and Zinszner B. 2004. Monitoring of CO_2 injected at Sleipner using time-lapse seismic data. *Energy* **29**, 1383–1392.

Calvert R. 2005. *Insights and Methods for 4D Reservoir Monitoring and Characterization*. EAGE/SEG Distinguished Instructor Short Course No. 8. SEG. ISBN 1560800860.

Castagna J.P., Batzle M.L. and Eastwood R.L. 1985. Relationships between compressional-wave and shear-wave velocities in clastic silicate rocks. *Geophysics* **50**, 571–581.

Drijkoningen G.G., Brouwer J., Kooijman J., Steenbergen G., Dost B. and Huijgen A. 2006. 4C seismic monitoring on land in the Netherlands – Results for acquisition design. 68^{th} EAGE meeting, Vienna, Austria, Expanded Abstracts, P291.

Geluk M. 2005. *Stratigraphy and tectonics of Permo-Triassic basins in the Netherlands and surrounding areas*. PhD thesis, Utrecht University.

Hatchell P.J. and Bourne S. 2005. Rock under strain: Strain-induced time-lapse time shifts are observed for depleting reservoirs. *The Leading Edge* **24**, 1222–1225.

Jeremic M.L. 1994. *Rock Mechanics in Salt Mining*. A.A. Balkema. ISBN 9054101032.

Kragh E. and Christie P. 2002. Seismic repeatability, normalized rms and predictability. *The Leading Edge* **21**, 640–647.

Landrø M. 2001. Discrimination between pressure and fluid saturation changes from time-lapse seismic data. *Geophysics* **66**, 836–844.

Schissele E., Forgues E., Echappé J., Meunier J., Pellegars O. de and Hubans C. 2009. Seismic repeatability – Is there a limit? 71st EAGE meeting, Amsterdam, the Netherlands, Expanded Abstracts, V021.

Urai J.L., Schléder Z., Spiers C.J. and Kukla P.A. 2008. Flow and transport properties of salt rocks. In: *Dynamics of Complex Intracontinental Basins*, *The Central European Basin System* (eds R. Littke, U. Bayer, D. Gajewski and S. Nelskamp), pp. 277–290. Springer. ISBN 3540850847.

Van Dalfsen W., Doornenbal J.C., Dortland S. and Gunnink J.L. 2006. A comprehensive seismic velocity model for the Netherlands based on lithostratigraphic layers. *Netherlands Journal of Geosciences* **85**, 277–292.

Virieux J. 1986. P-SV wave propagation in heterogeneous media: Velocity-stress finite difference method. *Geophysics* **51**, 889–890.